

## MANUFACTURING OF NANO/MICRO COMPOSITES USING FRICTION STIR PROCESSING

M. EL-SHENNAWY<sup>1</sup> & ADEL A. OMAR<sup>2</sup>

<sup>1,2</sup>Taif University, Engineering College, Department of Mechanical Engineering, Taif, KSA

<sup>1</sup>On Leave from Helwan University, Faculty of Engineering, Department of Mechanical Engineering,  
Helwan, Egypt

<sup>2</sup>On Leave from Benha University, Faculty of Engineering, Department of Mechanical Engineering Department,  
Benha, Egypt

### ABSTRACT

Compared with unreinforced metals, metal-matrix composites reinforced with ceramic phases exhibit high strength, high elastic modulus, and improved resistance to wear, creep and fatigue, which make them promising structural materials for aerospace and automobile industries. This article reviews various researches concerning the fabrication of nano and micro metal-matrix composites using the novel technique of friction stir processing, FSP.

**KEYWORDS:** Nano Composite, Metal-Matrix Composite, Aluminum-Matrix Composite, Friction Stir Process, Ceramic Particles, Novel Technique

### INTRODUCTION

Aluminum and its alloys are used extensively in aerospace and automotive industries because of its low density and high strength to weight ratio [1]. However, a poor resistance to wear and erosion is of serious concern for prolonged use [2]. Metal matrix composites are most promising new class of materials that exhibit good wear and erosion resistance properties, higher stiffness and hardness at a lower density as compared to the matrix [3]. This is due to the presence of nano and micro-sized reinforcement particles into the matrix. Aluminum matrix composites (AMCs) reinforced with particles and whiskers are widely used for high performance applications such as in automotive, military, aerospace and electricity industries because of their improved physical and mechanical properties [4]. In the composites relatively soft alloy like aluminum can be made highly resistant by introducing predominantly hard but brittle particles such as  $Al_2O_3$ . Hard particles such as  $Al_2O_3$  [5-15], SiC [16-26], TiC [27-31],  $TiO_2$  [32-34],  $Cr_2O_3$  [35,36], or mixture of them [37-40], and others [41-46] are commonly used as reinforcement in the composites. The application of  $Al_2O_3$  particle reinforced aluminum alloy matrix composites in the automotive and aircraft industries is gradually increasing for pistons, cylinder heads, connecting rods etc. where the tribological properties of the materials are very important [47-49]. However, the presence of the ceramic particles in the metallic matrix result in higher strength and hardness, often at the expense of some ductility [47] which makes the matrix brittle [50]. In this regard, it may however be noted that wear is a surface dependent degradation mode, which may be improved by a suitable modification of surface microstructure and/or composition [51]. Hence, instead of bulk reinforcement, if the ceramic particles would be added to the surface, it could improve the wear and erosion resistance without sacrificing the bulk properties [51]. The enhancement of mechanical properties in the novel nano-particle reinforced MMCs has been reviewed recently [4].

Dispersion of the nano-reinforcements particles on metallic substrate surface and the control of its distribution in a uniform manner is a critical and difficult to achieve by conventional surface treatments [52].

## FABRICATION OF METAL MATRIX COMPOSITES

### Conventional Methods

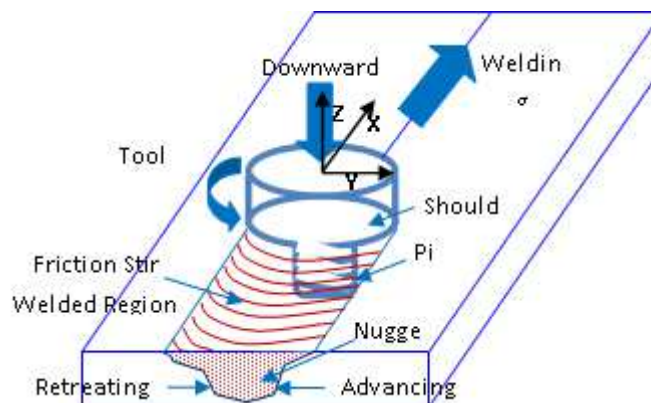
Fabrication of MMCs had been carried out using various methods. Those methods are based on surface modification techniques which include casting [53], cast sinter [54, 55], high-energy electron beam irradiation [56, 57], high-energy laser melt treatment [58-65], plasma spraying [66]. In Laser technique, metal-matrix composites using either carbide powder (SiC, TiC, or WC), or combination of carbide powders and a binding material (Co, Al, or Ni) could be obtained [59-63].

In the above mentioned techniques, it is hard to avoid the interfacial reaction between reinforcement and metal-matrix and the formation of some detrimental phases because these processing techniques are based on liquid phase processing at high temperatures. Furthermore, critical control of processing parameters is necessary to obtain ideal solidified microstructure in surface layer. Moreover, using conventional surface modification techniques makes it difficult to achieve successful dispersion of fine ceramic particles in a surface layer. Obviously, if processing of surface composite is carried out at temperatures below melting point of substrate, the problems mentioned above can be avoided.

### Friction Stir Processing Method

Recently, much attention has been paid to a new surface modification technique named friction stir processing (FSP) [67-70]. FSP is a solid state processing technique to obtain a fine-grained microstructure. It has been developed for microstructural modification by Mishra et al. [71, 72] based on the basic principles of friction stir welding (FSW).

FSW is a relatively new solid state joining process developed initially for aluminum alloys by The Welding Institute (TWI) of UK [73]. FSW uses a non-consumable rotating tool with a specially designed pin and shoulder is plunged into the interface between two plates to be joined and traversed along the line of the joint as shown in **Figure 1**.



**Figure 1: Principals of FSW**

Localized heating is produced by the friction between the rotating tool and the workpiece to raise the local temperature of the material to the range where it can be plastically deformed easily. As the rotating tool traverses along the joint line, metal is essentially extruded around the tool before being forged by the large down pressure [74-76]. It is well known that the stirred zone consists of fine and equiaxed grains produced due to dynamic recrystallization [76]. Though FSP has been basically advanced as a grain refinement technique, it is a very attractive process for also fabricating

composites. Mishra et al. [77] fabricated the Al/SiC surface composites by FSP, and indicated that SiC particles were well distributed in the Al matrix, and good bonding with the Al matrix was generated.

### **Nano/Micro Metal Matrix Composites**

Metal matrix composites containing nano-sized reinforcement particles inserted into the matrix are promising materials due to the enhancement in mechanical properties. Friction stir processing technique is used in manufacturing nano composites. Various reinforcement particles materials were applied in the metals matrices (metallic substrates) which were also varied from aluminum alloys to copper alloys and other easy friction stir processed metal alloy.

#### **Metallic Substrate**

##### **Aluminum Alloys**

Aluminum alloys are the most widely applied metallic substrate for producing nano composites [6, 8-10, 12, 16, 18, 19, 21, 22, 33-36, 41, 78, 79, 80-84]. There also applied in case of micro composites [5, 7, 11, 17, 20, 27, 28, 32, 37-39, 42, 85-87]. Aluminum alloy AA5083 [5, 17, 32, 38, 41, 85], AA1000 [6, 8, 10], AA6061 [18, 22, 36, 37, 39, 42, 81, 87], AA7075 [16, 19, 21, 35], AA6082 [9, 27, 28], A356 [11, 20, 78], and other aluminum alloys such as AA2618 [7], AA5052 [12] and aluminum magnesium alloy [33, 34, 82] were the most aluminum alloys received attention from researchers in the recent years concerning metal matrix composites.

##### **Other Metals and Alloys**

Copper was used as a metal substrate in manufacturing metal matrix composites [13, 88]. Magnesium [14], Titanium [23] and other alloys [43, 89] were also used as a metal substrate in producing metal matrix composites.

#### **Reinforcement Particle**

Alumina ( $\text{Al}_2\text{O}_3$ ) was the main reinforcement particle used with metal substrate regardless its type [5, 7-11, 13, 14, 78, 88]. Silicon carbide (SiC) was used extensively also as reinforcement particles with different metal matrices [16-23, 35, 84, 85]. Mixture of both  $\text{Al}_2\text{O}_3$  and SiC was also used [37-39]. Other carbides such as  $\text{TiC}$  [27, 28, 32], or oxides such as  $\text{TiO}_2$  [32-34] or  $\text{Cr}_2\text{O}_3$  [81] or compound such as Al-Cr-O [36] were applied as a reinforcement particles.

#### **Process and Joint Design**

There are various designs for the process followed for producing matrix metal composites MMCs using friction stir process, FSP and different designs for the joint or specimen used in this process. There are mainly two types of joint design followed in producing MMCs, first using flat plate [5, 8, 9, 12-15, 18, 20, 22-24, 26-28, 30-32, 34, 37-46, 90, 91], second using two plates to form a joint to be welded [16, 19, 21, 29]. In case of flat plate there were two main methods for inserting the reinforcement; first making groove(s) all through the plate length [8, 9, 12-15, 18, 20, 22-24, 27, 28, 32, 34, 37, 39-41, 43-46, 90, 91], second making holes in the substrate in two parallel line having specific distance apart between each line or each hole wall [26, 30, 31, 38, 42]. In case of the joint with two separate plates, groove was made at one edge of one plate and then been joined to the other plate [16, 19, 21, 29].

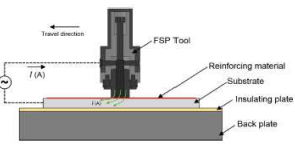
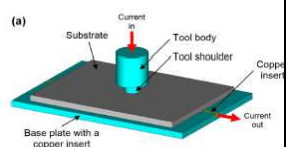
Tool used for FSP was mainly from hard steel alloy or tool steel such as H-13, or WC-Co alloy, ... etc. The tool design including shoulder diameter, pin shape and diameter(s) and length were varied to have columnar or conical shape which either threaded or un-threaded pin/probe.

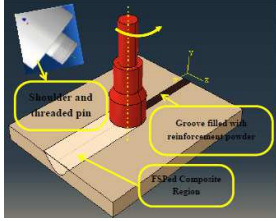
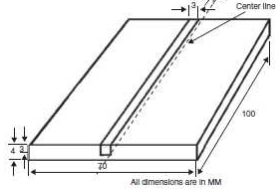
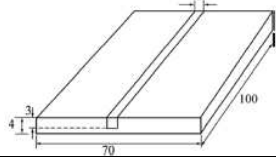
Friction stir process parameters were chosen according to the plate thickness, substrate material and tool used. Values varied in the range from 600 up to 1600 rpm for aluminum alloys, while traversing speed were in the range of 30 up to 180 mm/min [5, 8, 9, 37, 16, 36, 27, 18, 19, 20, 28, 39, 41, 21]. Special case was recorded using 3000 rpm and 348 mm/min for cylindrical specimen with holes [38]. For copper, it was 900-1000 rpm and 40-50 mm/min. In case of Mg and Mg alloys, it was 800-1500 rpm and 20-45 mm/min.

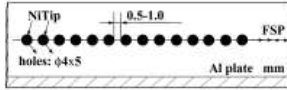
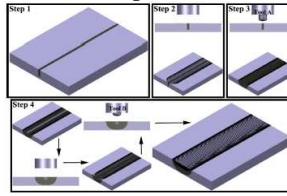
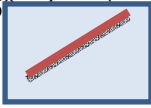
Material of substrate was mainly from aluminum and its alloys, copper, magnesium and its alloys. Some cases dealt with mild and stainless steel [29, 40] and titanium alloy [30, 43, 46].

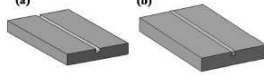
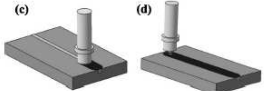
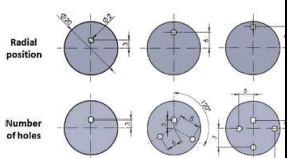


**Table 1** summarizes the above mentioned details concerning joint and process design extracted from numerous researches. It includes also material of substrate and reinforcement type used in those researches.

**Table 1: Various Process and Joint Designs According to Numerous Researches**


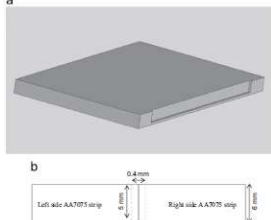
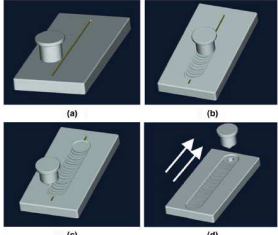
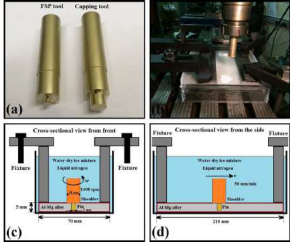
Substrate	Thickness, Mm	Rein- Forcement	Grai n Size, μM	Method	FSP Condition			Ref ·
					Joint Design	Travel Speed, Mm/ Min	Rotational Speed, Rpm	
AA5083-H111	8	Al <sub>2</sub> O <sub>3</sub>	45	<p>FSP Using electric current circuit 12V with 720A</p>  <p>Alumina: fixed with glue in spray Layers: several upto 200 μm thick.</p>		180	1120	5
		SiC & Al <sub>2</sub> O <sub>3</sub>	35 & 45	<p>FSP Tool: H-13 hardened tool steel with threaded concave pin, Shoulder: dia. 19 mm, tilt: 0 &amp; 2° Alumina: fixed with glue in spray. Layers: several upto 200 μm thick.</p>	---	180, 224, 355	1120, 710, 355, 1800	38

AA5083-O	5	Cerium Oxide and MWCNTs	30 and 0 respectively.	<p>FSP Tool: H-13 hot working tool steel and heat treated, Shoulder: cylindrical concave dia. 18 mm with threaded pin, Pin: dia. 6 mm, length 4.5 mm, Tilt: 5°, To prevent powder from spattering: tool with pinless shoulder was first used, Passes: 3 passes.</p>	<p>Groove dimensions: width x depth: 1.2 x 2 mm<sup>2</sup>.</p> 	35 (first 2 passes), 45 (last pass)	800 (first 2 passes), 600 (last pass)	41
AA6061-T6	4	SiC, Gr (graphite) & Al <sub>2</sub> O <sub>3</sub>	20	<p>FSP Tool: H-13 tool steel with screwed taper pin, Pin: dia. 8 mm, length 3.5 mm, Shoulder: dia. 24 mm, tilt: 2.5° Initial pass: shoulder without pin.</p>	<p>Groove dimensions: Square 3 x 3 mm<sup>2</sup>.</p> 	40 (5kN axial force)	900, 1120, 1400	37
		SiC+Gr, SiC+Al <sub>2</sub> O <sub>3</sub>		<p>FSP Tool: H-13, Shoulder: dia. 24 mm with screwed taper profile pin, Pin: dia. 8 mm, length 3.5 mm, Tilt: 2.5°. To prevent reinforcement escape: tool with shoulder without pin was used.</p>	<p>Groove dimensions: width x depth: 3 x 3 mm<sup>2</sup>. Tangential to the pin in the advancing side and 2 mm far away from the center line of the tool rotation on plate.</p> 	40	900	39
	13	Cr <sub>2</sub> O <sub>3</sub>	-	<p>FSP Tool: H-13, Shoulder: dia. 18 mm with threaded taper pin, Tilt: 3°, Pin: dia. 6 mm, length 4 mm, Reinforcement: placed by atmospheric plasma spray, Passes: 6.</p>	---			36
			20-40	<p>FSP Tool: H-13, Shoulder: dia. 18 mm with threaded conical pin, Pin: dia. 6 mm (upper), 4 mm (lower), length 4 mm, Tilt: 3°, Coating: 150 μm layer of Cr<sub>2</sub>O<sub>3</sub> was first coated by APS plasma system on substrate, Passes: 1-6 passes.</p>	No groove	100	630	81

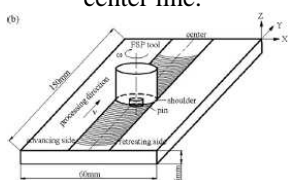
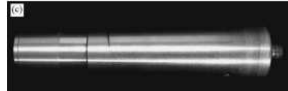
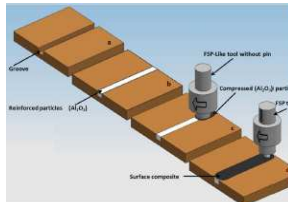
AA6061-O	-	Al <sub>2</sub> O <sub>3</sub>	0.320	<p>FSP</p> <p>Holes: 960 holes with dia. 1 mm and depth 2 mm in area 240 x 50 mm<sup>2</sup>,</p> <p>Filling: slurry of Al<sub>2</sub>O<sub>3</sub> was squeezed in the holes and dried in convection oven at 110°C for 2 hr,</p> <p>Tool:</p> <p>Shoulder: dia. 12.5 mm with threaded conical probe,</p> <p>Probe: dia. 5 mm and length 2 mm</p>	---	180 (3.6-4.2 kN axial force)	1200	10
AA6061-T651	6	NiTip	150-178, 2-74	<p>FSP</p> <p>Tool: M42 steel,</p> <p>Shoulder: dia. 24 mm with threaded pin,</p> <p>Pin: dia. 8, length 4.8 mm, Tilt: 2.7°,</p> <p>Reinforcement were compacted inside the hole with 5 MPa.</p>	<p>Groove dimensions: series of holes with dia 4 mm and depth 5 mm, wall thickness between holes: 0.5-1 mm.</p> 	100	600	42
AA6061	8	SiC	0.050	<p>FSP</p> <p>Tool: H-13 with two different pin profiles (threaded and square),</p> <p>Shoulder: dia. 20 mm,</p> <p>Pin: dia. 7.8 mm length 6 mm,</p> <p>Tilt: 3°,</p> <p>Reinforcement was packed in a groove with tool with shoulder only and no pin,</p> <p>Passes: single pass.</p> <p>Tool penetration: 0.12, 0.18, 0.24, 0.30 mm.</p>	<p>Groove dimensions: width x depth 1 x 5.9 mm<sup>2</sup>.</p>	40, 80, 125, 160	800, 1000, 1250, 1600	18
			0.050	<p>FSP</p> <p>Tool: H-13,</p> <p>Shoulder: dia. 20 mm with threaded pin,</p> <p>Pin: dia. 7.8 mm, length 6 mm (tool A) &amp; 3.2 mm (tool B),</p> <p>Tilt: 3°,</p> <p>To prevent powder from spattering: tool with pinless shoulder was used,</p> <p>Passes: 4 passes with cooling after each pass using tool A, then using tool B.</p>	<p>Groove dimensions: width x depth: 3 x 5.9 mm<sup>2</sup> with tool A and 2 x 2 mm<sup>2</sup> with tool B after the 4 passes.</p> 	40	1600	22
AA6082	7	Al <sub>2</sub> O <sub>3</sub>	0.05	<p>FSP</p> <p>Tool: Hardened H-13 tool steel,</p> <p>Shoulder: dia. 16 mm,</p> <p>Pin: dia. 5 mm, length 4 mm,</p> <p>Tilt: 3°.</p>	<p>Groove dimensions: width x length x depth: 1 x 16</p> 	135	1250	8

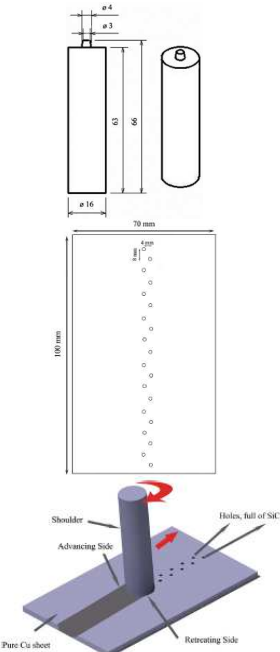
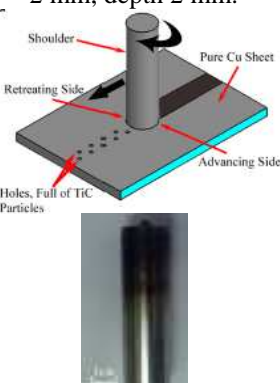
			50	Passes: 1-4	Groove dimensions: width x depth: 1 x 4 mm <sup>2</sup>		1000	9
				FSP Tool: H-13 tool steel Pin: dia. 5 mm, length 4 mm, Shoulder: dia. 16 mm, tilt: 3° Passes: 1-4 with cooling to room temp. after each pass, Initial pass: shoulder without pin.				
10	TiC	2	2	FSP Tool: HCHCr, Shoulder: dia. 18 mm with threaded pin, Pin: dia. 6 mm, length 5.5 mm, Reinforcement: pinless tool is used to cover the top of the groove after filling with TiC particles.\	Groove dimensions: 5 mm deep with 0, 0.4, 0.8, 1.2 and 1.6 mm width.  	60 (10 kN axial force)	1200	27
				FSP Tool: High Carbon High Chromium (HCHCr) oil hardened, Shoulder: dia. 22 mm with threaded pin, Pin: dia. 6 mm, length 5.5 mm.	Groove dimensions: width x depth: 0.8 x 5 mm <sup>2</sup> .			
AA6082-T6	20 mm dia. and 2 mm dia. holes	SiC	12.3	FSP		348 (7 kN axial force)	3000	38
AA7075-O	6		0.045 - 0.065	FSW Tool: H-13 (Hot working steel and heat treated), Shoulder: dia. 16 mm with threaded taper pin, Pin: length 5.7 mm, FSW for two strips.	Groove dimensions at adjoining side: width x depth: 0.2 x 5 mm <sup>2</sup> , Two strips are joined together 	30.5, 40, 50	800, 1000, 1250	16
				FSP Tool: H-13 heat treated with different pin geometries: threaded tapered, triangular, square, four-flute square, and four-flute cylindrical,	Groove dimensions at adjoining side: width x depth: 0.2 x 5 mm <sup>2</sup> , Two strips are joined together 	40	1250	19

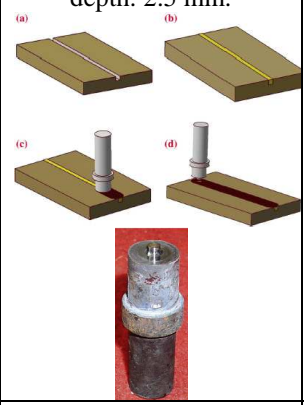
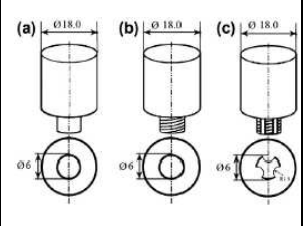


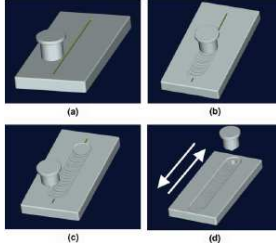
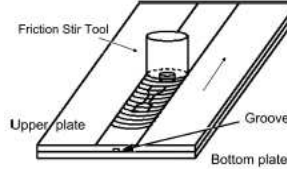
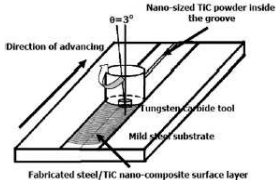
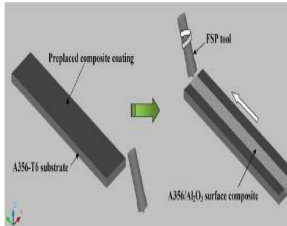
				Pin: dia. 4-6 and length 5.7 mm.				
AA7075	6			FSP Tool: H-13 hot worked with threaded tapered pin.	Groove dimensions: width x depth: 0.2 x 5 mm <sup>2</sup> on the faying surface of each plate. 			21
AA5052-H32	4	Al <sub>2</sub> O <sub>3</sub>	0.050	FSP Tool: H-13, Shoulder: dia. 13.6 mm, Pin: dia. 5, length 3.7, Tilt: 2.5 – 5° Passes: 2 – 4 without stop (no time for cooling), To prevent powder from spattering: Tool with pinless shoulder was used.	Groove dimensions: width x depth: 1 x 2 mm <sup>2</sup> . 	Rotational speed/travel speed: 8 – 100 mm/rev.		12
	5	TiO <sub>2</sub>	0.030	FSP Tool: dia. 18 mm having concave shape with threaded cylindrical pin, Pin: dia. 5 mm, length 4 mm, Tilt: 2.5°C, To fill powder: tool with pinless shoulder (capping tool) was used, Passes: 1-4 passes.	Groove dimensions: width x depth: 1.2 x 4 mm <sup>2</sup> .	30 (first pass), 100	1075 (first pass), 1200	34
AA5052	5			FSP Tool: H-13 with a concave shoulder, Shoulder: dia. 18 mm, Pin: dia. 5 mm, length 4, Tilt: 2.5°, To close the groove: tool with pinless shoulder (capping tool, shoulder dia. 12 mm) was used in first pass, Media: different cooling atmospheric; air (ambient), water-dry ice mixture (~0°C) and liquid nitrogen (~-196 °C).	Groove dimensions: width x depth: 1.2 x 3.5 mm <sup>2</sup> . 	30 (first pass), 50-200	1125 (first pass), 800-1400	33

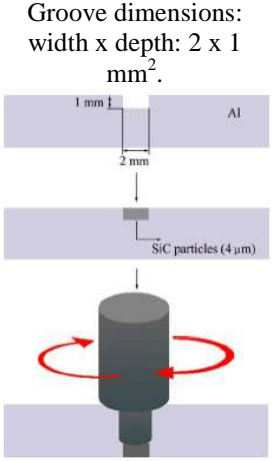
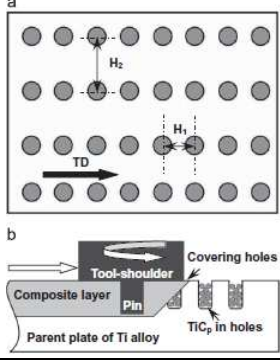


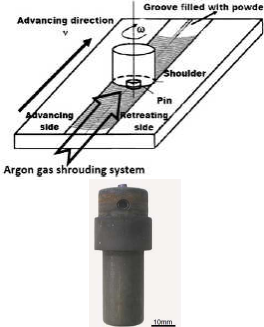
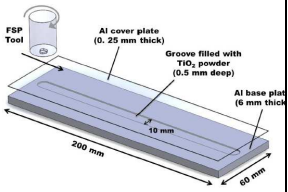
AA2618-T6	7	Al <sub>2</sub> O <sub>3</sub> 20%		FSP Tool: powder metallurgy with 50% TiC.	---	250	750	7
AA1050	5	SiC	10	FSP Tool: AISI 1050, Shoulder: dia. 25 mm without pin and inserted 0.1 mm into the workpiece, Tilt: 2°, Passes: single pass.	---	15, 20, 30	500, 700, 1000	17
Al-10SiO <sub>2</sub>	12	Al <sub>2</sub> O <sub>3</sub> resulted after FSP	0.02	FSP Shoulder: dia. 16 mm, Pin: dia. 6 mm x 1.2 mm pitch, 6 mm length, Tilt: 3°, Passes: multiple with cooling to room temp. after each pass.	---	15 - 90	500 - 2000	6
Al-Si10Mg	5	SiC 30 Vol. %	-	FSW Tool: WC-Co hard alloy, Shoulder: dia. 13.6 with threaded columnar pin, Pin: 6dia. 6 mm, length 4.85 mm, Backing: stainless steel.	No Groove.	25, 50, 100, 150	2000	25
5A06Al (Al-Mg alloy)	6	SiCp	10	FSP Tool: high-speed steel, Shoulder: columnar shape dia. 18 mm with screwed pin, Pin: dia. 6 mm, Tilt: 2.5°.	Groove dimensions: width x depth: 0.5 x 1 mm <sup>2</sup> . The groove was 2.8 mm far from the center line.  	95	1180	91
Pure Cu	3	Al <sub>2</sub> O <sub>3</sub>	20	FSP Tool: H-13, Shoulder: dia. 24 mm, with square pin, Pin: dia. 8, length 2 mm, Passes: single pass. To prevent powder from escaping: tool with pinless shoulder was used.	Groove dimensions: it was made in the advancing side 1 mm far away from the center line of the tool rotation on the substrate, the groove size varied along with the volume percentage 4, 8 & 12%. 	40	900	13

	5	SiC	25	<p>FSP                  Tool: shoulder dia. 16 mm with conical pin,                  Pin: dia. 3 &amp; 4 mm, length 3 mm,                  Tilt: 3°,                  Net of holes was used for filling the reinforcement.</p>	<p>Groove dimensions: No groove. Net of holes was used with zigzag shape having 4 mm distance between holes' center in transverse direction and 8 mm in longitudinal direction.</p> 	50	1000	26
	6	TiC		<p>FSP                  Tool with shoulder dia. 16 mm with conical pin,                  Pin: dia. 4 &amp; 3 mm, length 3 mm,                  To prevent reinforcement from scattering: Tool with pinless shoulder was used.</p>	<p>Groove dimensions: no groove. Holes were drilled along the surface of the substrate. Hole dia. 2 mm, depth 2 mm.</p> 			31

		B <sub>4</sub> C	4	<p>FSP                      Tool: double tempered hot working steel,                      Shoulder: dia. 20 mm,                      Pin: dia. 5 mm, length 3 mm,                      To prevent scattering of reinforcement: Tool with pinless shoulder was used.</p>	<p>Groove dimensions:                      depth: 2.5 mm.</p> 	40 (10 kN axial force)		45
Pure Mg	5	Hydroxyapatite, HA	5	<p>FSP                      Tool: H-13 tool steel,                      Shoulder: dia. 15 mm with tapered pin,                      Pin: dia. 3 &amp; 5 mm, length 2.7 mm.</p>	<p>Groove dimensions:                      width x depth: 1 x 2 mm<sup>2</sup>.</p>	12 (5000 N load)	1200	44
AZ31	6	Al <sub>2</sub> O <sub>3</sub> CNTs	0.050 0.030	<p>FSP                      Tool with shoulder dia. 20 mm and conical pin,                      Pin: dia. 5.5 &amp; 3.5 mm, length 5 mm,                      Tilt: 0.5°,                      Passes: 4 passes,                      To seal the groove: Tool with pinless shoulder was used.</p>	<p>Groove dimensions:                      width x depth: 2 x 5 mm<sup>2</sup>.</p>	33.4	1050	14
	10	Al <sub>2</sub> O <sub>3</sub>	0.035, 0.350, 1.0	<p>FSP                      Tool: H-13,                      Shoulder: dia. 18 mm,                      Pin: dia. 6 mm, length 5.7 mm (3 pin types columnar without threads, columnar with threads and columnar with threads and three flutes,                      Tilt: 2°,                      To prevent reinforcement from being displaced: Tool with pinless shoulder was used,                      Passes: 2-4 passes, advancing direction for the subsequent pass was in the opposite direction to the previous pass.</p>	<p>Groove dimensions:                      width x depth: 1.2 x 5 mm<sup>2</sup>.</p> 	45	800, 1000, 1200	15

AZ61A		SiO <sub>2</sub>	0.020	<p>FSP                      Tool: with shoulder dia. 18 mm,                      Pin: dia. 6 mm, length 6 mm,                      Tilt: 2°,                      Cooling: using back plate with 3 cooling channels with cooling water,                      Passes: 1-4 passes,                      To prevent reinforcement from displacing: tool with pinless shoulder was used.</p>	<p>Groove dimensions:                      width x depth: 1.25 x 6 mm<sup>2</sup> (1 and 2 grooves were used).</p> 	800	90	
AZ63	4	SiC	0.040	<p>FSP                      Tool with shoulder dia. 20 mm,                      Pin: dia. 6 mm length 4.2 mm,                      Tilt: 2.5°,                      Passes: 5 passes,                      After filling the powder, another plate in the same size with no groove was put upon the first plate, and then the two plates were put upside down.</p>	<p>Groove dimensions:                      width x depth: 2 x 2 mm<sup>2</sup>.</p> 	20	1500	24
Mild Steel		TiC	0.070	<p>FSW                      Tool: Tungsten Carbide,                      Shoulder: dia. 16 mm,                      Pin: 5 mm,                      Tilt: 3°,                      Hole was drilled on groove beginning to decrease tool wear,                      Passes: 1-4 passes.</p>	<p>Groove dimensions:                      width x depth: 1 x 2 mm<sup>2</sup>.</p> 	31.5	1120	29
A356-T6	10	Al <sub>2</sub> O <sub>3</sub>	50-100 & 0.020 - 0.040	<p>Mechanical milling, High Velocity Oxy-fuel (HVOF) Spraying and FSP                      High energy planetary ball mill for A356-5 vol% Al<sub>2</sub>O<sub>3</sub>,                      Sieving milled powder to 25-63 μm,                      HVOF spraying to deposit the powder onto the grit blasted A356-T6                      FSP Tool: H-13,                      Tilt: 2°.</p>		200	1600	11

A356	4	SiC	4	<p>FSP Tool: H-13, Shoulder: columnar with threaded pin, To prevent the sputtering of powder: aluminum tape is used to close the gap, Passes: double pass (back side and front side).</p>		127	1800	20
SS 304	--	SiC (reactive) & Al <sub>2</sub> O <sub>3</sub> (non-reactive)	2-3 & 0.5	<p>FSP Tool: WC-Co alloy, Shoulder: columnar dia. 12 mm, Pin: dia. 7 mm, length 2.4 mm, Fill the groove: Plane tool with 12 mm dia. Under lower load was used.</p>	<p>Groove dimensions: width x depth: 1 1 mm<sup>2</sup>.</p>	1000 (1000 kgf constant load)	100	40
Ti-6Al-4V	3	Hydroxyapatite, HA	nano	<p>FSP Tool: Tungsten carbide, dia. 16 mm, Tilt: 3°, To prevent the stir zone and tool from oxidizing: argon gas shrouding system was used, Max temp: 850-900 °C.</p>	<p>Groove dimensions: width x depth: 2 x 1 mm<sup>2</sup> (3 grooves separated from each other by a 2 mm distance).</p>	16	250	43
		TiC	5.5	<p>FSP Tool: WC-13 wt% Co, Shoulder: dia. 15 mm with tapered pin, Pin: 4 &amp; 6 mm, length 2.2 mm, Filling the reinforcement: through numerous blind-holes, Passes: multi passes, Shielding: Ar2 gas surrounding the rotating tool and upper the processed zone to prevent oxidation, Temp.: ~ 1100 °C.</p>	<p>Groove dimensions: no grooves. Numerous blind holes were drilled, dia. 1 mm, depth 0.5 – 2 mm.</p> 	---	---	30
		Hydroxyapatite, HA	nano	<p>FSP Tool: tungsten carbide dia. 16 mm, Tilt: 3°, Passes: 3 passes under argon gas shrouding system.</p>	<p>Groove dimensions: 3 grooves separated 2 mm from each other: width x depth: 2 x 1 mm<sup>2</sup>.</p>	16	250	46

CP-Ti	6	SiC	0.050	<p>FSP            Tool: H-13 with pin made of tungsten carbide,            Shoulder: dia. 28 mm,            Pin: dia. 6 mm, length 3 mm,            Tilt: 0°,            Using argon shrouding system.            Passes: 1-4 passes.</p>	<p>Groove dimensions:            width x depth: 2 x 2 mm<sup>2</sup>.</p> 	25 - 65	600 - 1600	23
Peraluman™ 853		TiO <sub>2</sub>	0.210	<p>FSP            Tool: Steel,            Shoulder: dia. 20 mm with threaded pin,            Pin: dia. 6, length 1.5 mm,            Tilt: 1°,            To prevent loss of TiO<sub>2</sub>:            filled plates were covered by the same Al sheet with 0.25 mm thickness,            Passes: 7 passes.</p>	<p>Groove dimensions:            width x depth x length:            10 x 0.5 x 180 mm<sup>3</sup>.</p> 	200 (1 <sup>st</sup> pass), 1000 (subsequent passes)	1000	32

## Examinations

Metallurgical and mechanical characteristics of metal matrix composites were studied extensively by researchers to evaluate the effect of adding and inserting the reinforcement particles to the matrix. Examinations were carried out to study the effects of many factors on mechanical and metallurgical characteristics of the composite. Those factors include volume percent of the reinforcement [13, 27, 45, 85], number of passes [12, 23, 29, 33, 92], tool design [15, 18, 19, 80, 92], process parameters such as rotational and traverse speeds [15, 18, 25, 93]. The effect of using mixture of reinforcements had been also investigated [14, 37-41]. There were some researches which dealt with the friction stir process as a cure for the previously produced composites by other methods such as powder metallurgy [82, 83], laser cladding [89, 93], and stir casting [92, 94]. The effect of reinforcement in general was the dominating factor studied. The main reinforcements used for producing the composites were Al<sub>2</sub>O<sub>3</sub> [5-15, 39] and SiC [16-26] or mixture of them [37-40]. Other oxides or carbides of titanium have been also used as reinforcements [27-34].

## Metallurgical

Optical and scanning examinations [5-10, 12-14, 16-23, 27, 28, 32-39, 41-43, 78-89] and x-ray diffraction [11] in some cases were the main analysis techniques followed to determine the metallurgical properties. Main results of using FSP and nano/micro reinforcements showed grain refinement and even distribution of reinforcements [10, 12-15, 17, 19, 21, 23, 25-31, 33, 34, 40, 41, 44-46, 81, 82, 84, 87, 88, 90-95]. Grain refinement and better distribution of the reinforcement played the main role for enhancement of mechanical properties in general including wear rate decrease and hardness increase as explained below. The grain refinement was also enhanced with increasing both number of passes and tool rotational speed. The FSP cured the problem of grain growth associated with stir casting or laser cladding by breaking down the carbides resulted after those processes. In the same time eliminated the porosities existed after the process of stir

casting. It was also noticed that intermetallic compounds were not existed neither in the SZ nor in the TMAZ which helped in strengthening the composite and homogenizing its properties all through.

### **Mechanical**

Mechanical properties were measured through tensile test, hardness test, wear test [5-14, 16-20, 22, 23, 27, 28, 32-39, 41-43, 78-89] and in limited cases fatigue and impact tests [21]. The main results indicated increases in hardness/microhardness and consequently wear resistance [5, 8-11, 14, 15, 17, 19, 20, 22-24, 26-28, 30, 33, 37, 40, 41, 45, 46, 78, 80, 81, 87, 89-93], mechanical properties including yield strength, ultimate tensile strength [6, 10, 12, 13, 16, 18, 19, 21, 27, 33, 35, 37, 41, 78-81, 90, 92, 95], compression strength [78, 82], bending strength [17, 46], elongation [12, 16, 21, 33, 42, 81, 95], ductility [6, 16, 34, 35, 79] and stiffness [27], fatigue life [7, 21], toughness [21] and impact strength [13, 21]. Mechanical properties were affected directly by the metallurgical characteristics as explained above. Grain refinement and uniform distribution of the reinforcement were the reasons behind the enhancement of the mechanical properties including hardness and wear resistance. Tensile properties were also improved including yield and tensile strength, in the same time elongation and ductility. In specific cases compression and bending strength were measured and showed better records after FSP. It is worth noting that all wear tests of material composites showed abrasive wear mainly.

### **CONCLUSIONS**

Friction stir process is used recently as a surface modification method. It has the advantage of being solid-state process where the melting point of the material is not reached. The superplasticity condition of the stirred zone encouraged many researchers use it in manufacturing the metal composites where substrate is being grooved and reinforcement is put inside it, then the FSP is applied. This reinforcement is either in micro or nano size. The resulted microstructure has specific characteristics metallurgical and mechanical. The researchers studied the effect of various factors on such characteristics. Those factors were mainly concentrated on the reinforcement volume percentage, the reinforcement and substrate material, the process conditions such as number of passes, tool design and rotational and traverse speeds. The results can be summarized in the following points:

- Friction stir process showed grain refinement and improved mechanical properties such as yield and ultimate tensile strength, compressive and bending strength, toughness and fatigue life, and hardness, wear and corrosion resistance.
- Main reinforcements applied for composite manufacturing were SiC and Al<sub>2</sub>O<sub>3</sub>, whether the substrate material was aluminum or its alloys or other material such as copper or steel.
- Hybrid reinforcement where two types were used had shown good results concerning microstructure and mechanical properties.
- Increasing number of passes or tool rotational speed showed more microstructure refinement and better mechanical properties for the composite.
- Threaded tool was the best among other tool designs like three-flute or non-threaded design where fine microstructure and higher mechanical properties were recorded.
- Friction stir process could improve the resulted microstructure of metal composites manufactured by other



methods like stir casting or laser cladding where large grains have been broken into fine grains and porosities were limited after FSP application.

## REFERENCES

1. H. Bakes, D. Benjamin, C. W. Kirkpatrick (Eds.), *Metals Handbook*, vol. 2, ASM, Metals Park, OH, 1979, pp. 3–23.
2. Y. Wan, Q. J. Xue, *Tribol. Lett.* 2 (1996) 37–45.
3. M. E. Smagorinski, P. G. Tsantrizos, S. Grenier, *J. Min. Met. Mater.* 48 (1996) 56–59.
4. Sajjadi SA, Ezatpour HR, Beygi H., *Proceedings of 14th national conference on Materials Science and Engineering*, Tehran, Iran; 2010. pp. 325–32.
5. Telmo G. Santos, N. Lopes, Miguel Machado, Pedro Vilaca, R. M Miranda, *J Mat. Proc. Tech.* 216 (2015), pp. 375-380.
6. You, G. L., Ho, N. J., Kao, P. W., *Mat. Charact.* 80 (2013), pp. 1-8.
7. Cavaliere, P, *Composites, Part A* 36 (2005), pp. 1657-1665.
8. Shafiei-Zarghani, A, Kashani-Bozorg, S. F., Zarei-Hanzaki, A, *Wear* 270 (2011), pp. 403-412.
9. Shafiei-Zarghani, A, Kashani-Bozorg, S. F., Zarei-Hanzaki, A, *Mater. Sci. Engg. A* 500 (2009), pp. 84-91.
10. Guo, J. F., Liu, J, Sun, C. N., Maleksaedi, S., Bi, G., Tan, M. J., Wei, J., *Mater. Sci. Engg. A* 602 (2014), pp. 143-149.
11. Mazaheri, Y., Karimzadeh, F., Enayati, M. H., *J. Mater. Proc. Tech.* 211 (2011), pp. 1614-1619.
12. Sharifitabar, M. Sarani, A. Khorshahian, S. Shafiee Afarani, M., *Materials and Design* 32 (2011), pp. 4164–4172.
13. Suvarna Raju, L., Kumar, A., *Proc. Mater. Sci.* 5 (2014), pp. 434-443.
14. Dehong Lu, Yehua Jiang, Rong Zhou, *Wear* 305 (2013), pp. 286–290.
15. Azizieh, M., Kokabi, A. H., Abachi, P., *Materials and Design* 32 (2011), pp. 2034–2041.
16. Mohsen Bahrami, Kamran Dehghani, Mohammad Kazem Besharati Givi, *Materials and Design* 53 (2014), pp. 217–225.
17. Adem Kurta, Ilyas Uygurb, Eren Cete, *Jl. Mater. Proc. Tech.* 211 (2011), pp. 313–317.
18. Salehi, M., Saadatmand, M., Aghazadeh mohandesi, J., *Trans. Nonferrous Met. Soc. China* 22 (2012), 1055-1063.
19. Mohsen Bahrami, Mohammad Kazem Besharati Givi, Kamran Dehghani, Nader Parvin, *Materials and Design* 53 (2014), 519–527.
20. Don-Hyun Choi, Yong-Hwan Kim, Byung-Wook Ahn, Yong-Il Kim, Seung-Boo Jung, *Trans. Nonferrous Met. Soc. China* 23 (2013), pp. 335–340.
21. Mohsen Bahrami, Nader Helmi, Kamran Dehghani, Mohammad Kazem Besharati Givi, *Mat. Sci. & Engg. A* 595 (2014), pp. 173–178.

22. Mojtaba Salehi, Hamidreza Farnoush, Jamshid Aghazadeh Mohandesi, *Materials and Design* 63 (2014), pp. 419–426.
23. Ali Shamsipur, Seyed Farshid Kashani-Bozorg, Abbas Zarei-Hanzaki, *Surface & Coatings Technology* 206 (2011), pp. 1372–1381.
24. Sun, K., Shi, Q. Y., Sun, Y. J., Chen, G. Q., *Mat. Sci. and Engg. A* 547 (2012), pp. 32–37.
25. Huijie Liu, Yanying Hu, Yunqiang Zhao, Hidetoshi Fujii, *Materials and Design* 65 (2015), pp. 395–400.
26. Akramifard, H. R., Shamanian, M., Sabbaghian, M., Esmailzadeh, M., *Materials and Design* 54 (2014), pp. 838–844.
27. Thangarasu, A., Murugan, N., Dinaharan, I., Vijay, S. J., *Archives of Civil and Mechanical Engineering* 15 (2015), pp. 324–334.
28. Thangarasu, A., Murugan, N., Dinaharan, I., Vijay, S. J., *Procedia Mat. Sci.* 5 (2014), pp. 2115–2121.
29. Ahmad Ghasemi-Kahrizsangi, Seyed Farshid Kashani-Bozorg, *Surface & Coatings Technology* 209 (2012), pp. 15–22.
30. Bo Li, Yifu Shen, Lei Luo, Weiye Hu, *Mat. Sci. & Engg. A* 574 (2013), pp. 75–85.
31. Sabbaghiana, M., Shamaniana, M., Akramifarda, H. R., Esmailzadeh, M., *Ceramics International* 40 (2014), pp. 12969–12976.
32. Visweswara Chakravarthy Gudla, Flemming Jensen, Aude Simar, Rajashekhara Shabadi, Rajan Ambat, *Applied Surface Science* 324 (2015), pp. 554–562.
33. Khodabakhshi, F., Gerlich, A. P., Simchi, A., H. Kokabi, A., *Mat. Sci. & Engg A* 620 (2014), 471–482.
34. Khodabakhshi, F., Simchi, A., Kokabi, A. H., Gerlich, A. P., Nosko, M., *Materials and Design* 63 (2014), pp. 30–41.
35. Mohsen Bahrami, Kamran Dehghani, Mohammad Kazem Besharati Givi, *Materials and Design* 53 (2014), pp. 217–225.
36. Anvari, S. R., Karimzadeh, F., Enayati, M. H., *Wear* 304 (2013), pp. 144–151.
37. Devaraju Aruria, Kumar Adepua, Kumaraswamy Adepub, Kotiveerachari Bazavada, *J. Mat. Res. Tech.* 2 (2013), pp. 362–369.
38. Miranda, R. M., Santosa, Telmo G., Gandrab, J., Lopesa, N., Silva, R. J. C., *Jl. Mat. Proc. Tech.* 213 (2013), pp. 1609–1615.
39. Devaraju, A., Kumar, A., Kotiveerachari, B., *Trans. Nonferrous Met. Soc. China* 23 (2013), pp. 1275–1280.
40. Kimoto, Y., Nagaoka, T., Watanabe, H., Fukusumi, M., Osaka Municipal Technical Research Institute, Japan, pp. 389–393.
41. Hossieni, S. A., Khalil Ranjbar, Dehmlaei, R., Amirani, A. R., *Jl. Alloys and Compounds* 622 (2015), pp. 725–733.

42. Ni, D. R., Wanga, J. J., Zhou, Z. N., Ma, Z. Y., *Jl. of Alloys and Compounds* 586 (2014), pp. 368–374.
43. Hamidreza Farnousha, Ashkan Abdi Bastamia, Ali Sadeghib, Jamshid Aghazadeh Mohandesia, Fathollah Moztarzadeh, *Jl. Mech. Behavior of Biomedical Materials* 20 (2013), pp. 90–97.
44. Sunil, B. Ratna, Kumar, T. S. Sampath, Uday Chakkingal, Nandakumar, V., Mukesh Doble, *Mat. Sci. and Engg. C39* (2014), pp. 315–324.
45. Sathiskumara, R., Murugana, N., Dinaharanb, I., Vijay, S. J., *Mat. Characterization* 84 (2013), pp. 16–27.
46. Hamidreza Farnoush, Ali Sadeghi, Ashkan Abdi Bastami, Fathollah Moztarzadeh, Jamshid Aghazadeh Mohandesi, *Ceramics International* 39 (2013), pp. 1477–1483.
47. Vencel A, Bobic I, Arostegui S, Bobic B. Structural, mechanical and tribological properties of A356 aluminum alloy reinforced with Al<sub>2</sub>O<sub>3</sub>, SiC and SiC + graphite particles. *J. Alloys Compd.* 506 (2010), pp. 631–639.
48. Sajjadi SA, Torabi Parizi M, Ezatpour HR, Sedghi A. Fabrication of A356 composites reinforced with micro and nano Al<sub>2</sub>O<sub>3</sub> particles by a developed compocasting method and study of their properties. *J. Alloys Compd.* 511 (2012), pp. 226-231.
49. Mazahery A, Abdizadeh H, Baharvandi HR. Development of high-performance A356/nano-Al<sub>2</sub>O<sub>3</sub> composites. *Mater Sci Eng A* 518 (2009), pp. 61–64.
50. T. W. Clyne, P. J. Withers, *An Introduction to Metal Matrix Composites*, Cambridge University Press, Cambridge, 1993.
51. E. Rabinowicz, *Friction and Wear of Materials*, John Wiley and Sons, New York, 1965.
52. K. G. Budinski, *Surface Engineering for Wear Resistance*, Prentice-Hall, New Jersey, 1988.
53. A. N. Attia, *Mater. Des.* 22 (2001), 451.
54. Y. Wang, X. Zhang, G. Zeng, F. Li, *Mater. Des.* 21 (2000), 447.
55. Y. S. Wang, X. Y. Zhang, G. T. Zeng, F. C. Li, *Composites Part A* 32 (2001), 281.
56. S.-H. Choo, S. Lee, S.-J. Kwon, *Metall. Mater. Trans. A* 30A (1999), 1211.
57. S.-H. Choo, S. Lee, S.-J. Kwon, *Metall. Mater. Trans. A* 30A (1999), 3131.
58. G. Ricciardi, M. Cantello, G. Mollino, W. Varani, E. Garlet, *Proceedings of 2nd International Seminar on Surface Engineering with High Energy Beam, Science and Technology, CEMUL-IST, Lisbon, Portugal, 1989*, pp. 415-423.
59. D. Pantelis, A. Tissandier, P. Manolatos, P. Ponthiaux, *Mater. Sci. Technol.* 11 (1995), 299.
60. C. Hu, T. N. Baker, *J. Mater. Sci.* 30 (1995), 891.
61. C. Hu, H. Xin, T. N. Baker, *J. Mater. Sci.* 30 (1995), 5985.
62. C. Hu, H. Xin, T. N. Baker, *Mater. Sci. Technol.* 12 (1996), 227.
63. C. Hu, T. N. Baker, *J. Mater. Sci.* 32 (1997), 5047.

64. T. C. Lei, J. H. Ouyan, Y. T. Pei, Y. Zhou, *Mater. Sci. Technol.* 11 (1995), 520.
65. L. R. Katipelli, N. B. Dahotre, *Mater. Sci. Technol.* 17 (2001), 1061.
66. M. C. Gui, S. B. Kang, *Mater. Lett.* 46 (2000), 296.
67. H. J. Liu, H. Fujii, K. Nogi, *Mater. Sci. Technol.* 20 (2004), pp. 399–402.
68. K. Ohishi, T. R. Mcnelley, *Metall. Trans. A* 35A (2004), pp. 2951–2961.
69. J. Q. Su, T. W. Nelson, C. J. Sterling, *Scripta Mater.* 52 (2005), pp. 135–140.
70. D. C. Hofmann, K. S. Vecchio, *Mater. Sci. Eng. A* 402 (2005), pp. 234–241.
71. R. S. Mishra, M. W. Mahoney, S. X. McFadden, N. A. Mara, A. K. Mukherjee, *Scripta Mater.* 42 (2000), 163.
72. R. S. Mishra, M. W. Mahoney, *Mater. Sci. Forum* 507 (2001), pp. 357-359.
73. W. M. Thomas, E. D. Nicholas, J. C. Needham, M. G. Murch, P. Templesmith, C. J. Dawes, G. B. Patent Application No. 9125978.8, December 1991.
74. K. Colligan, *Weld. J.* 78 (1999), pp. 229S–234S.
75. T. U. Seidel, A. P. Reynolds, *Metall. Mater. Trans. A* 32A (2001), pp. 2879–2887.
76. R. S. Mishra, Z. Y. Ma, *Mater. Sci. Eng. R* 50 (2005), pp. 1–78.
77. R. S. Mishra, Z. Y. Ma, I. Charit, *Mater. Sci. Eng. A* 341 (2003), pp. 307–310.
78. Sajjadi, S. A., Ezatpour, H. R., Torabi Parizi, M., *Materials and Design* 34 (2012), pp. 106–111.
79. Patrick B. Berbon, William H. Bingel, Rajiv S. Mishra, *Scripta Mater.* 44 (2001), pp. 61–66.
80. Qiang Liu, Liming Ke, Fencheng Liu, Chunping Huang, Li Xing, *Materials and Design* 45 (2013), pp. 343–348.
81. S. R. Anvari, F. Karimzadeh, M. H. Enayati, *J. Alloys and Compd* 562 (2013), pp. 48–55.
82. You, G. L., Ho, N. J., Kao, P. W., *Materials Letters* 100 (2013), pp. 219–222.
83. Wang, D., Xiao, B. L., Wang, Q. Z., Ma, Z. Y., *J. Mater. Sci. Technol.* 30 (2014), pp. 54-60.
84. Arash Heydarian, Kamran Dehghani, Taymor Slamkish, *Metall. And Mat. Trans. B* 45 (2014), pp. 821-826.
85. Izadi, H., Noltingb, A., Munrob, C., Bishopc, D. P., Plucknettc, K. P., Gerlich, A. P., *Jl. of Mat. Proc. Tech.* 213 (2013), pp. 1900–1907.
86. Ma, Z Y., Liu, Z Y., Zhang, Q., Ni, D R., Xiao, B L., *Proc. of the 1st Int. Joint Symp.on Joining and Welding* (2013), pp. 395-399.
87. Dinaharan, I., Ashok Kumar, G., Vijay, S. J., Murugan, N., *Materials and Design* 63 (2014), pp. 213–222.
88. Suvarna Raju, L., Kumar, A., *Defence Technology* 10 (2014), pp. 375-383.
89. Ruidi Li, Tiechui Yuan, Zili Qiu, Kechao Zhou, Jinglong Li, *Surface & Coatings Technology* 258 (2014), pp. 415–425.

90. Lee, C. J., Huang, J. C., Hsieh, P. J., *Scripta Materialia* 54 (2006), pp. 1415–1420.
91. Wei Wang, Qing-yu Shi, Peng Liu, Hong-ke Li, Ting Li, *Jl. of Mat. Proc. Tech.* 209 (2009), pp. 2099–2103.
92. Vijayavel, P., Balasubramanian, V., Sundaram, S., *Materials and Design* 57 (2014), pp. 1–9.
93. Ruidi Li, Tiechui Yuan, Zili Qiu, *Applied Surface Science* 308 (2014), pp. 176–183.
94. Ni, D. R., Xiao, B. L., Ma, Z. Y., Qiao, Y. X., Zheng, Y. G., *Corrosion Science* 52 (2010), pp. 1610–1617.
95. Zhu, S J., Jin, J., Wang, J., Sun, Y F., Chen, J., Wang, L G., Fujii, H., Guan, S K., *Proc. of the 1st Int. Joint Symp. on Joining and Welding* (2013), pp. 411-415.